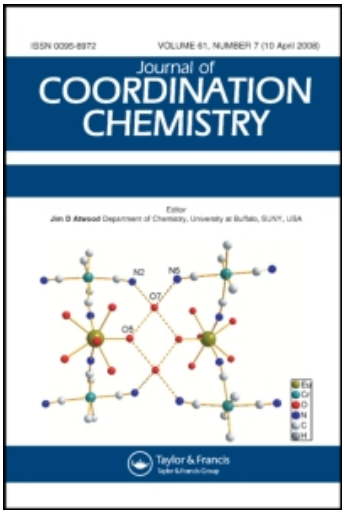

Journal of Coordination Chemistry
Publication details, including instructions for authors and subscription information:
http://www.informaworld.com/smpp/title~content=t713455674

Synthesis, crystal structure and properties of bis(hexafluoroacetylacetonato)tetrazinecopper(II)

Lixin Li[a]; Christopher P. Landee[b]; Mark M. Turnbull[a]; Brendan Twamley[c]
[a] Carlson School of Chemistry and Biochemistry, Clark University, Worcester, MA 01610, USA [b] Department of Physics, Clark University, Worcester, MA 01610, USA [c] University Research Office, University of Idaho, Moscow, ID 83844, USA

To cite this Article Li, Lixin , Landee, Christopher P. , Turnbull, Mark M. and Twamley, Brendan(2006) 'Synthesis, crystal structure and properties of bis(hexafluoroacetylacetonato)tetrazinecopper(II)', Journal of Coordination Chemistry, 59: 12, 1311 — 1320
To link to this Article: DOI: 10.1080/09553000500515525
URL: http://dx.doi.org/10.1080/09553000500515525

Journal of Coordination Chemistry
Vol. 59, No. 12, 5 August 2006, 1311–1320

Synthesis, crystal structure and properties of bis(hexafluoroacetylacetonato)tetrazinecopper(II)

LIXIN LI†, CHRISTOPHER P. LANDEE‡,
MARK M. TURNBULL*† and BRENDAN TWAMLEY§

†Carlson School of Chemistry and Biochemistry, Clark University,
Worcester, MA 01610, USA
‡Department of Physics, Clark University, Worcester, MA 01610, USA
§University Research Office, University of Idaho, Moscow, ID 83844, USA

(*Received 11 August 2005; in final form 28 November 2005*)

A new complex bis(hexafluoroacetylacetonato)tetrazinecopper(II), $Cu(hfac)_2(tetz)$ (**1**), has been prepared by reaction of $Cu(hfac)_2 \cdot xH_2O$ and 1,2,4,5-tetrazine in CH_2Cl_2. Orange crystals suitable for X-ray diffraction analysis of **1** were obtained by slow evaporation at room temperature. Complex **1** crystallizes in the triclinic space group $P\bar{1}$, with $a = 11.4825(7)$, $b = 13.4950(8)$, $c = 13.8328(8)$ Å, $\alpha = 104.990(1)$, $\beta = 111.888(1)$, $\gamma = 94.245(1)^\circ$, $V = 1886.23(19)$ Å^3, $R_1 = 0.0507$ based on 6814 independent reflections. The complex is unstable at room temperature and decomposes with loss of the tetz ligand. Differential scanning calorimetry (DSC) and magnetic properties are reported.

Keywords: Bis(hexafluoroacetylacetonato)tetrazinecopper(II); 1,2,4,5-Tetrazine; DSC; Magnetic susceptibility; Crystal structure

1. Introduction

Electronic interactions, especially magnetic exchange interactions, between transition metal ions linked by bridging groups are part of an old, active and heavily explored field, although still full of challenging problems [1]. The use of diazines, such as pyrazine, pyrimidine, quinoxaline, and phenazine, as bridging ligands has a long history in coordination chemistry and magnetochemistry [2–4]. Pyrazine (pz) and its derivatives especially, in spite of their low basicity (for pyrazine $pK_{a1} = 0.65$ [5]), are widely used as bridging bidentate ligands giving rise to dimers, such as $[(NH_3)_5Ru(II)\text{-pz-}Ru(III)(NH_3)_5]$ [4] and linear chains, such as $[Cu(hfac)_2 \cdot pz]$ [6]. Hatfield and co-workers studied the magnetism of two related linear chain copper(II) complexes with pyrazine bridges. In the coordination polymer $[Cu(hfac)_2(pz)]_n$, no superexchange interaction was observed in the magnetic susceptibility data down to 1.8 K [7]. The absence of exchange interaction was attributed to the fact that the

*Corresponding author. Email: mturnbull@clarku.edu

Journal of Coordination Chemistry
ISSN 0095-8972 print: ISSN 1029-0389 online © 2006 Taylor & Francis
DOI: 10.1080/09553000500515525

pyrazine plane lies in the *xz* plane of the $Cu(hfac)_2$ unit, where the copper(II) ground state is $d_{x^2-y^2}$ and there is no effective π-orbital pathway available on the pyrazine. On the other hand, the pyrazine-bridged coordination polymer $[Cu(pz)(NO_3)_2]$ [7] has shown antiferromagnetic chain-like behavior which was described by the Heisenberg linear-chain model [8]. In this case, the pyrazine groups lie canted about 50° from the copper *xy* plane, which allows for $d_{x^2-y^2}$–π (b_{1g}) overlap and leads to a π-orbital pathway for pyrazine superexchange interactions. We are interested in the effect of using 1,2,4,5-tetrazine (tetz) instead of pyrazine on metal–metal superexchange interactions. The obvious attraction of tetrazine for coordination chemistry lies in its potential for multiple metal binding sites. Chains or layers will be expected if two or four nitrogen atoms take part in the coordination, respectively. The general topic of coordination chemistry of 1,2,4,5-tetrazines has been recently reviewed [9]. Several complexes with 3,6-disubstituted tetz derivatives were synthesized and studied by powder X-ray diffraction [9]. No structures have been reported for complexes of neutral tetz as a ligand, however, a crystal structure of the Ti(IV) complex of the corresponding dianion has been reported [10]. A few compounds of tetz have been characterized by IR or NMR techniques [11]. Perhaps the difficulty in synthesis and the thermal and photochemical instability of tetz itself have contributed to the relative scarcity of well-defined coordination compounds of tetz and its derivatives.

We have long been interested in the synthesis of new low-dimensional magnetic systems and have prepared and studied a number of linear chain [12–14] and square layer systems [15, 16]. We report here the synthesis, structure, thermal properties and powder magnetic susceptibility of bis(hexafluoroacetylacetonato)tetrazinecopper(II), $Cu(hfac)_2$(tetz) (**1**).

2. Experimental

All reagents were obtained from Aldrich or Fluka and used without further purification. FT-IR-spectra were recorded using KBr pellets on a Perkin Elmer Paragon 500 Spectrometer (4000–450 cm^{-1}) or using a carefully selected orange crystal (for complex **1**) on an IlluminatIR manufactured by Smithes Detection and coupled to an Olympus BX-50 microscope (4000–650 cm^{-1}). ^1H NMR and ^{13}C NMR spectra of the ligand tetrazine were recorded on a Bruker 200 MHz spectrometer at room temperature using $CDCl_3$ as solvent and TMS as internal standard.

2.1. *Synthesis*

2.1.1. 1,2,4,5-Tetrazine, $C_2H_2N_4$. 1,2,4,5-Tetrazine was synthesized from formamidine acetate and hydrazine monohydrate in a one-pot procedure [17]. Hydrazine monohydrate (30.10 g, 0.60 mol) was added dropwise to formamidine acetate (30.05 g, 0.29 mol) in 50 mL MeOH with stirring at 0°C. Glacial acetic acid (95.0 mL) was added slowly over a period of about 90 min at 0–10°C. Then, solid $NaNO_2$ (37.54 g, 0.544 mol) was added to the reaction mixture in small portions, maintaining the reaction system below 10°C. Stirring was continued for 1 h at 10°C and then for another 1 h at room temperature. Finally, solid $NaHCO_3$ (62.15 g, 0.74 mol) and

water (65 mL) were added and the stirring was continued for 30 min at room temperature. The resulting red suspension was vacuum filtered to remove undissolved $NaHCO_3$. The filtrate was extracted with CH_2Cl_2 (10×25 mL). The combined organic extracts were washed with saturated aqueous $NaHCO_3$ (3×25 mL) and water (25 mL) and dried over $CaCl_2$. The solvent was evaporated at room temperature in the dark. The resulting red solid was purified immediately by sublimation (bath 10°C, cold finger −56°C, 0.1 Torr). Yield: 1.405 g (12%). m.p. 96–97°C. IR: 3084(m, sharp), 2942(w), 2401(w), 1885(m), 1445(s), 1201(s), 1148(m), 1105(s), 887(s). ^{1}H NMR ($CDCl_3$): δ 10.4(s). ^{13}C NMR($CDCl_3$): δ 161.

2.1.2. Cu(hfac)$_2 \cdot x$H$_2$O. The complex Cu(hfac)$_2 \cdot x$H$_2$O was prepared according to the literature method [18] and used without further purification. m.p: 120–124°C. IR: 3683(m, sharp), 3563(w, sharp), 1645(s), 1612(m), 1563(m), 1536(m), 1467(s), 1255(vs), 1217(s, broad), 1148.2(vs), 1108(s), 807(s), 747(m), 680(s), 597(m), 529(w).

2.1.3. Cu(hfac)$_2$(C$_2$H$_2$N$_4$). A solution of tetz (0.082 g, 1.0 mmol) in 12 mL CH_2Cl_2 was added dropwise to a stirred solution of Cu(hfac)$_2 \cdot x$H$_2$O (0.512 g, 1.0 mmol) in 40.0 mL CH_2Cl_2. The resulting dark brown solution was stirred for another 0.5 h, followed by filtration. Orange crystals were harvested after evaporation of almost all of the solvent at room temperature for one day. Yield: 0.402 g (72%). IR: 1642(m), 1608(w), 1563(w), 1531(w), 1469(m), 1431(w), 1196(m), 1130(vs), 1102(s), 896(m), 803(m), 746(w), 678(m), 666(w).

2.2. *Crystal structure determination*

Crystals of compound **1** were removed from their container, a suitable crystal was selected, attached to a glass fiber and data were collected at 298(2) K using a Bruker/Siemens SMART APEX instrument (Mo Kα radiation, $\lambda = 0.71073$ Å) equipped with a Cryocool NeverIce low temperature device. Data were measured using omega scans of 0.3° per frame for 5 s, and a full sphere of data was collected. A total of 2450 frames were collected with a final resolution of 0.83 Å. The first 50 frames were recollected at the end of data collection to monitor for decay. Cell parameters were retrieved using SMART [19] software and refined using SAINTPlus [20] on all observed reflections. Data reduction and correction for Lp and decay were performed using the SAINTPlus software. Absorption corrections were applied using SADABS [21]. The structure was solved by direct methods and refined by least squares on F^2 using the SHELXTL program package [22]. All non-hydrogen atoms were refined anisotropically. The fluorine atoms of the CF_3 groups exhibit large thermal displacements, suggesting some disorder in their positions. Attempts at modeling these with disordered/split positions led to poorer refinements. No decomposition was observed during data collection. Details of the data collection and refinement are given in table 1. Further details are provided in the Supporting Information.

Table 1. Crystal data and structure refinement for **1**.

Empirical formula	$C_{48}H_{16}Cu_4F_{48}N_{16}O_{16}$
Formula weight	2238.93
Temperature (K)	298(2)
Wavelength (Å)	0.71073
Crystal system	Triclinic
Space group	$P\bar{1}$
a (Å)	11.4825(7)
b (Å)	13.4950(8)
c (Å)	13.8328(8)
α (°)	104.990(1)
β (°)	111.888(1)
γ (°)	94.245(1)
Volume (Å^3)	1886.23(19)
Z	1
Density (calculated) (mg m^{-3})	1.971
Absorption coefficient (mm^{-1})	1.304
$F(000)$	1092
Crystal size (mm^3)	$0.58 \times 0.42 \times 0.26$
θ range for data collection (°)	1.59 to 25.25
Index ranges	$-13 \le h \le 13$, $-16 \le k \le 16$, $-16 \le l \le 16$
Reflections collected	21372
Independent reflections	6814 [R(int) = 0.0230]
Max. and min. transmission	0.713 and 0.508
Solution method	XS, Bruker SHELXTL v. 6.12
Refinement method	Full-matrix least-squares on F
Data/restraints/parameters	6814/0/598
Goodness-of-fit on F^2	1.065
Final R* indices [$I > 2\sigma(I)$]	$R_1 = 0.0507$, $wR_2 = 0.1451$
R indices (all data)	$R_1 = 0.0566$, $wR_2 = 0.1508$
Largest diff. peak and hole (e Å^{-3})	0.940 and −0.598

*$R_1 = \sum||F_o| - |F_c||/\sum|F_o|$; $wR_2 = \{\sum[w(F_o^2 - F_c^2)^2]/\sum[w(F_o^2)^2]\}^{1/2}$.

2.3 *Stability studies and magnetic measurements*

Thermal decomposition studies were carried out on a Perkin Elmer DSC 7 over the temperature range 25–135°C, at a heating rate of 10°C min^{-1}. Magnetic susceptibility data were measured on a Quantum Design MPMS XL SQUID magnetometer. Crystals of complex **1** were powdered and packed into a #3 gelatin capsule. There was no hysteresis observed in the magnetization of the sample as a function of applied field from 0 to 5 T at 1.8 K. The moment is linear with the applied field up to at least 15000 Oe. Susceptibility data were taken over the temperature range from 1.8 to 325 K in an applied field of 1000 Oe. The data were corrected for temperature-independent paramagnetism and for the diamagnetism of the constituent atoms using Pascal's constants.

3. Result and discussion

3.1. *Structure description*

Complex **1** crystallizes in the triclinic space group $P\bar{1}$. Its molecular geometry and atomic numbering are shown in figure 1. Selected bond lengths and angles are listed in table 2.

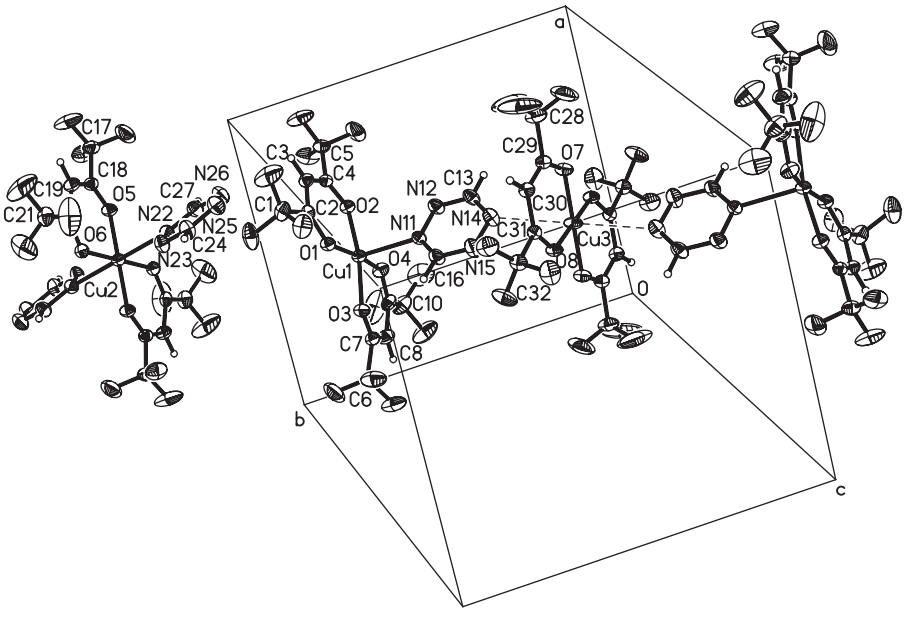

Figure 1. Thermal ellipsoid (20% probability level for clarity of overall structure) drawing of the complex $[Cu(hfac)_2(C_2H_2N_4)]_4$. Only the asymmetric unit is labeled (hydrogen and fluorine atom labels are omitted for clarity).

In each unit cell, there are four Cu(II) ions with three different coordination modes. Cu1 is bonded to four oxygen atoms from two independent hfac ligands and a nitrogen atom from a tetz ligand, forming a distorted square pyramid (figure 2a). The base of this square pyramid consists of four oxygen atoms with a mean deviation 0.011 Å from that plane. Cu1 is shifted 0.18 Å above this plane. In this way, an inverted umbrella structure is formed. The bond lengths Cu1–O1, Cu1–O2, Cu1–O3 and Cu1–O4 are normal [23], varying from 1.927(2) to 1.953(3) Å, but the Cu1–N11 bond length is 2.343(3) Å, which is longer than the average for Cu–N coordination bonds [24] and implies that the tetz molecule is weakly coordinated to the metal. Cu2 sits on an inversion center and is also bonded to four oxygen atoms from two hfac ligands, but unlike Cu1, it coordinates with two nitrogen atoms from two different tetz ligands, forming a six-coordinate distorted octahedron (figure 2b). Cu2 is in the center and the distances Cu2–O5, Cu2–O6 are similar (1.948(2) Å, 1.962(2) Å respectively). However, along the axial direction, the Cu2–N22 distance is longer (2.466(3) Å), which again implies that the tetz molecules are weakly coordinated to the metal, and the bond length disparity is likely a result of a Jahn–Teller distortion. This agrees with the observed facile loss of tetz from the complex. Cu3 also lies on an inversion center and is coordinated with four oxygen atoms from two hfac ligands, forming a nearly square planar structure with Cu3 in the center. In addition, two nitrogen atoms from different tetz molecules lie in the axial sites, but with a Cu3–N14 distance of 2.817(4) Å, too long to be considered as a true coordination bond (see figure 2c). Certainly, there is an intermolecular interaction of some type; the distance is shorter than the sum of their van der Waals radii.

Table 2. Selected bond lengths (Å) and angles (°) for **1**.

Cu1–O1	1.938(2)	Cu1–O2	1.927(2)
Cu1–O3	1.953(3)	Cu1–O4	1.944(3)
Cu1–N11	2.343(3)	Cu2–O5	1.948(2)
Cu2–O6	1.962(2)	Cu2–N22	2.466(3)
Cu3–O7	1.925(2)	Cu3–O8	1.931(2)
C1–F1*	1.322(5)	C1–F2	1.277(6)
C1–F3	1.346(6)	C2–O1	1.256(4)
C4–O2	1.255(4)	C7–O3	1.257(5)
C9–O4	1.234(5)	N11–N12	1.313(4)
N12–C13	1.331(6)	C13–N14	1.329(6)
N15–N14	1.307(5)	N15–C16	1.334(6)
C16–N11	1.302(5)	C18–O5	1.256(5)
C20–O6	1.240(5)	N22–N23	1.329(5)
N23–C24	1.306(6)	C24–N25	1.313(6)
N25–N26	1.304(7)	N26–C27	1.336(7)
C27–N22	1.304(6)	C29–O7	1.249(4)
C31–O8	1.253(4)		
O2–Cu1–O1	92.28(10)	O2–Cu1–O4	86.54(11)
O1–Cu1–O4	170.38(12)	O2–Cu1–O3	169.04(12)
O1–Cu1–O3	87.59(11)	O4–Cu1–O3	91.75(12)
O2–Cu1–N11	96.87(11)	O1–Cu1–N11	93.99(11)
O4–Cu1–N11	95.64(12)	O3–Cu1–N11	94.07(11)
O5–Cu2–O6	91.71(11)	O5–Cu2–N22	90.68(11)
O6–Cu2–N22	95.52(11)	O7–Cu3–O8	92.69(10)
C16–N11–Cu1	124.4(2)	N12–N11–Cu1	117.8(2)
C27–N22–Cu2	131.6(3)	N23–N22–Cu2	111.7(2)
C2–O1–Cu1	125.0(2)	C4–O2–Cu1	125.3(2)
C7–O3–Cu1	125.2(3)	C9–O4–Cu1	125.6(3)
C18–O5–Cu2	124.5(2)	C20–O6–Cu2	124.2(2)
C29–O7–Cu3	123.8(2)	C31–O8–Cu3	123.7(2)
N11–N12–C13	116.4(3)	N14–C13–N12	125.9(4)
N14–N15–C16	117.0(3)	N11–C16–N15	126.1(4)
C24–N23–N22	116.4(4)	N23–C24–N25	127.3(5)
N25–N26–C27	116.7(4)	N22–C27–N26	126.3(5)

*Representive C–F bond lengths are given.

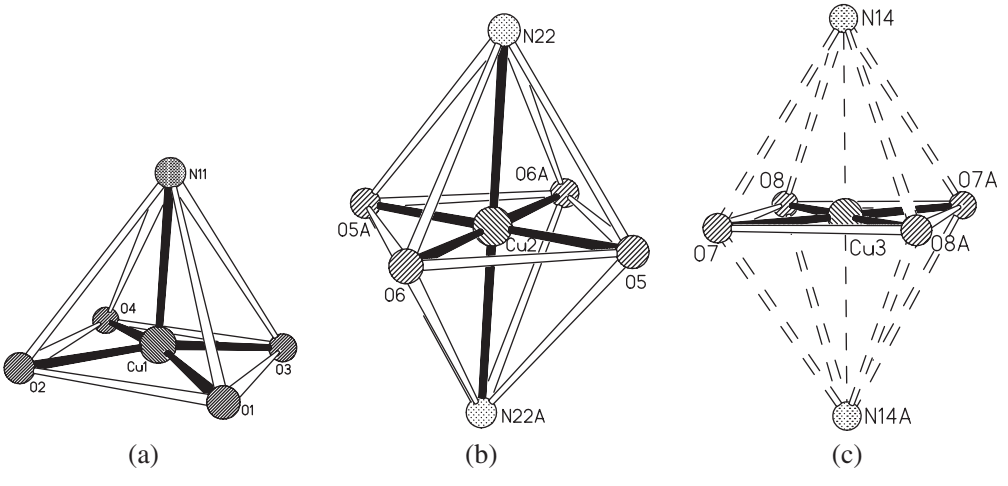

Figure 2. The copper coordination polyhedra. (a) five coordination for Cu1; (b) six coordination for Cu2; (c) four coordination for Cu3 with a weak interaction between center atom Cu3 and the axial nitrogen atoms (denoted by dash lines).

It is interesting to compare the two chemically equivalent, but crystallographically independent tetz molecules. The asymmetric unit can be divided into a trimeric part and a monomeric part. In the trimeric part, the tetz ring binds to Cu1 through N11 (distance = 2.343(3) Å), and it also bridges to Cu3 through a weak interaction between N14 and Cu3 (distance = 2.817(3) Å). Thus, the tetz ring behaves as a pseudo-bidentate ligand in the trimeric unit. On the other hand, in the monomeric unit the tetz ring coordinates with Cu2 only through N22 (distance = 2.466(3) Å), as a monodentate ligand. The uncoordinated end of this ring could potentially occupy the vacant coordination site on Cu1, but the shortest distance between Cu1 and this tetz ring is 4.902(4) Å (via N26), too far to be considered as any type of interaction. The differences between corresponding bond lengths and angles of the two rings are very small (less than 0.015 Å, or 1°) and usually within experiment error. In addition, the difference in bond lengths and angles between tetz itself [25] and the tetz rings in compound **1** are on the same order; another indication that the coordination is weak.

Throughout the structure, all the carbon and oxygen atoms in the same hfac moiety are planar with a maximum mean deviation of 0.03 Å. Also, the tetz molecules are planar with a maximum mean deviation of 0.01 Å; angles between the tetz ring and the Cu-hfac planes range from 75.2 to 86.4°. This is in distinct contrast to the structure of the reported titanocene derivative [10] where the tetrazine dianion rings are highly distorted, as expected for the reduced ligand. The tetz dianion is a much stronger ligand, as would be expected due to its increased electron density, and exhibits stronger coordination characteristics as seen in the much shorter M–N bond lengths [$d_{Ti-N} = 2.028(5)$ and 2.132(5) Å].

A packing diagram of **1** is shown in figure 3. Through the weak interaction between the tetz ligand and copper, the five-coordinated Cu1 is connected with a four-coordinated Cu3 which again connects with another five-coordinated copper, forming a trimeric unit. On the other hand, in its coordination to Cu2, the tetz behaves as a monodentate ligand, forming an octahedral unit. The desired chain or layer structures are not obtained due to the poor coordination ability of the ligand.

3.2. *DSC study*

DSC data show two endotherms at low temperature. One smaller endothermic process occurred at 48°C and the second larger endotherm occurred at 67°C. No endotherm was observed near the melting point of the tetz ligand (95–99°C). Above 70°C, the DSC curve agrees with the behavior of pure $Cu(hfac)_2 \cdot xH_2O$ with a large endotherm observed at 117°C.

It is interesting to consider the coordination ability of the tetz. Compared with pyridine ($pK_a = 5.3$), pyrazine is a weaker base ($pK_a = 0.65$) [5] because of its more uniform distribution of electron density to the two nitrogen atoms compared to the one nitrogen atom in the pyridine. For the same reason, tetrazine has four nitrogen atoms and only two carbon atoms. The electron cloud from the polar C–N bonds can be evenly distributed over the four nitrogen atoms. As a result, tetrazine is expected to be a weaker base and poorer electron donor than pyrazine. This is probably why there are few coordination complexes of tetrazine reported in the literature. Indeed, attempts to prepare related complexes of tetrazine with $CuBr_2$, $Cu(NO_3)_2$,

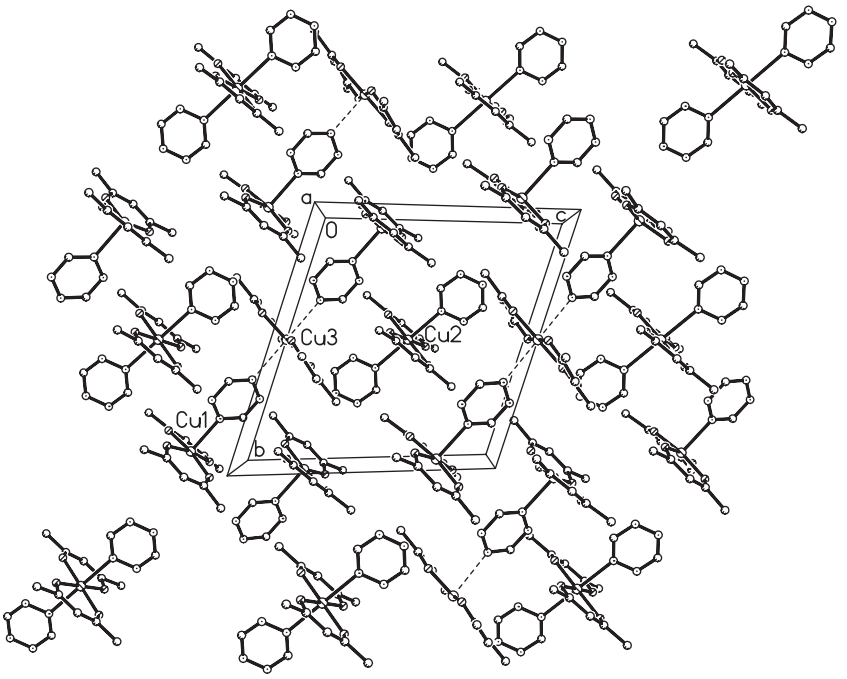

Figure 3. Packing diagram of **1**, viewed parallel to the *a* axis (hydrogen and fluorine atoms are omitted for clarity).

$CuCl_2$, $Cu(ClO_4)_2$, $Cu(acac)_2$ were unsuccessful. A tetz complex could only be isolated with the use of the strong Lewis acid $Cu(hfac)_2$.

The poor coordination ability of tetz is also reflected by the thermal stability of the complex. At room temperature, tetrazine sublimes readily and decomposes photochemically. The two endothermic peaks at 48 and 67°C from the DSC studies of **1** can be attributed to the loss of tetrazine due to the weak interaction of the ligand with the metal. The dissociation of tetrazine can be also verified by the observed color change. When the complex was heated in air, a color change from orange to green [the characteristic color of $Cu(hfac)_2 \cdot xH_2O$] was observed, beginning just above room temperature. The change was completed by 81°C. When the temperature was raised above 81°C, a further color change from green to brown was observed. The remaining $Cu(hfac)_2$ began to melt at 117°C, in agreement with the large endotherm observed in the DSC data.

3.3. *Magnetic properties*

Magnetization data as a function of field were collected for complex **1** at 1.8 K from 0 to 5 Tesla. A smooth curve was obtained and the long moment varied linearly with the applied field up to 15 kOe. Magnetization data as a function of temperature were collected at 1000 Oe from 1.8 to 325 K. Figure 4 shows the results plotted as χ *versus* T and χT *versus* T. No maximum was observed in χ *versus* T and the χT product is virtually constant over the entire temperature range, indicating a lack of internal

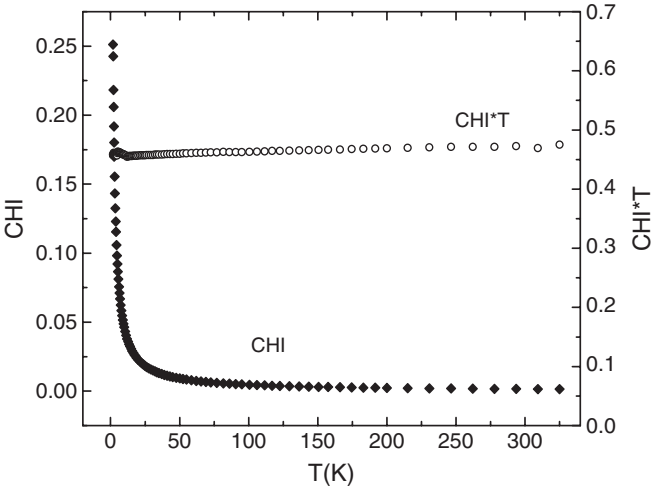

Figure 4. Magnetic susceptibility *vs.* temperature (CHI *vs.* T (K)) and CHI * T *vs.* temperature (K) for **1**.

exchange interactions. It is a paramagnetic material with a Curie constant of 0.465 at high temperature, slightly higher than expected for a Cu(II) compound with $S = 1/2$.

The calculated g value for **1** is 2.23 from the observed Curie constant. This is a little high if compared with ideal tetrahedral structure of Cu(II) complex ($g = 2.0023$ for T_d). If we consider the complicated structure of **1** with different coordination polyhedrons and geometry, it is not unexpected to obtain a higher g value. Similar examples have been reported previously [26]. Furthermore, the dissociation and loss of some tetz at room temperature during sample preparation would also contribute a higher observed Curie constant when the magnetic data were processed using the molecule weight of the pure material.

4. Conclusions

The new complex bis(hexafluoroacetylacetonato)tetrazinecopper(II), characterized by X-ray diffraction, DSC analysis and magnetic susceptibility measurements, represents the first structure of a complex containing neutral tetz as a ligand. Tetz is a poor ligand and exhibits weak interactions with the metal. As a result, it is easily lost from the complex even at room temperature, as verified by the DSC study. Magnetic data show the complex is a paramagnetic material without significant exchange interactions.

Supplementary data

Crystallographic data for the structure reported in this article have been deposited in the Cambridge Crystallographic Data Center, CCDC No. 276447. Copies of the

data can be obtained free of charge on application to CCDC, 12 Union Road, Cambridge CB2 1EZ, UK (e-mail: deposit@ccdc.cam.ac.uk).

Acknowledgements

The Quantum Design MPMS XL SQUID magnetometer was established at Clark University with the assistance of funds from the National Science Foundation (IMR-0314773) and a donation from PolyCarbon Ind., Inc. The Bruker (Siemens) SMART APEX diffraction facility was purchased by University of Idaho with the assistance of the NSF-EPSCoR program and the M.J. Murdock Charitable Trust, Vancouver, WA, USA. We also acknowledge the Andrew W. Mellon Foundation whose generous grants to the Worcester Art Museum (WAM) in Massachusetts provided funding for the purchase of the FT-IR micro-spectrometer unit (IIIuminatIR) used in the WAM Conservation Department.

References

[1] (a) R.D. Willet, D. Gatteschi, O. Kahn (Eds). *Magneto-structural Correlations in Exchange Coupled Systems*, Reidel, Dordrecht, Holland (1985); (b) R.L. Carlin. *Magnetochemistry*, Springer-Verlag, Berlin (1986); (c) O. Kahn. *Molecular Magnetism*, VCH Publishers, New York (1993); (d) L.J. de Jongh (Ed.). *Magnetic Properties of Layered Transition Metal Compounds*, Kluwer Acad. Pub., Dordrecht (1990); (d) M.M. Turnbull, T. Sugimoto, L.K. Thompson (Eds). *Molecule-Based Magnetic Materials: Theory, Techniques and Applications*, ACS Symposium Series #644, American Chemical Society, Washington (1996).
[2] J.F. Villa, W.E. Hatfield. *J. Am. Chem. Soc.*, **93**, 4081 (1971).
[3] D.B. Losee, H.W. Richardson, W.E. Hatfield. *J. Chem. Phys.*, **59**, 3600 (1973).
[4] C. Creutz, H. Taube. *J. Am. Chem. Soc.*, **95**, 1086 (1973).
[5] A. Chia, R.F. Trimble Jr. *J. Phys. Chem.*, **65**, 863 (1961).
[6] R.C.E. Belford, D.E. Fenton, M.R. Truter. *J. Chem. Soc., Dalton Trans.*, 17, (1974).
[7] H.W. Richardson, J.R. Wasson, W.E. Hatfield. *Inorg. Chem.*, **16**, 484 (1977).
[8] J.C. Bonner, M.E. Fisher. *Phys. Rev.*, **135**, A640 (1964).
[9] W. Kaim. *Coord. Chem. Rev.*, **230**, 127 (2002).
[10] S. Kraft, E. Hanuschek, R. Beckhaus, D. Haase, W. Saak. *Chem. Eur. J.*, **11**, 969 (2005).
[11] M. Herberhold, M. Süess-Fink. *Z. Naturforsch.*, **31B**, 1489 (1976).
[12] P.R. Hammar, M.B. Stone, D.H. Reich, C. Broholm, P.J. Gibson, M.M. Turnbull, C.P. Landee, M. Oshikawa. *Phys. Rev. B*, **59**, 1008 (1999).
[13] C.P. Landee, M.M. Turnbull. *Mol. Cryst. Liq. Cryst.*, **335**, 905 (1999).
[14] S. Amaral, W.E. Jensen, C.P. Landee, M.M. Turnbull, F.M. Woodward. *Polyhedron*, **20**, 1317 (2001).
[15] F.M. Woodward, A.S. Albrecht, C.M. Wynn, C.P. Landee, M.M. Turnbull. *Phys. Rev. B*, **65**, 144412 (2002).
[16] M.M. Turnbull, A.S. Albrecht, G.B. Jameson, C.P. Landee. *Mol. Cryst. Liq. Cryst.*, **335**, 957 (1999).
[17] D.K. Heldmann, J. Sauer. *Tetrahedron Lett.*, **38**, 5791 (1997).
[18] J.A. Bertrand, R.I. Kaplan. *Inorg. Chem.*, **5**, 489 (1966).
[19] *SMART: v.5.626, Bruker Molecular Analysis Research Tool*, Bruker AXS, Madison, WI (2002).
[20] *SAINTPlus: v.6.36a, Data Reduction and Correction Program*, Bruker AXS, Madison, WI (2001).
[21] *SADABS: v.2.01, An Empirical Absorption Correction Program*, Bruker AXS Inc., Madison, WI (2001).
[22] G.M. Sheldrick. *SHELXTL: v.6.10, Structure Determination Software Suite*, Bruker AXS Inc., Madison, WI (2001).
[23] Y.-B. Dong, M.D. Smith, R.C. Layland, H.-C. Zur Loye. *Inorg. Chem.*, **38**, 5027 (1999).
[24] S. Amaral, M.M. Turnbull. *J. Chem. Crystallogr.*, **32**, 11 (2002).
[25] F. Bertinotti, G. Giacomello, A.M. Liquori. *Acta Cryst.*, **9**, 510 (1956).
[26] H.W. Richardson, W.E. Hatfield. *J. Am. Chem. Soc.*, **98**, 835 (1976).